DIRAC Report

SPSC – October 2021

L. Nemenov on behalf of the DIRAC Collaboration

Outline

1. Investigation of $\pi^+\pi^-$, $K^+\pi^-$ and $K^-\pi^+$ atoms.
2. K^+K^- pairs analysis in the effective mass region near $2m_{K.}$
3. Proton-antiproton pairs analysis preliminary results.
4. The first evaluation of the K^+K^- atom numbers.
5. The short-lived $\pi^+\pi^-$ atom lifetime measurement.

Outline

Investigation of $\pi^+\pi^-$, $K^+\pi^-$ and $K^-\pi^+$ atoms.

1.The first short-lived $\pi^+\pi^-$ atom lifetime measurement and $\pi\pi$ scattering length evaluation.

2. The first long-lived $\pi^+\pi^-$ atom observation and its lifetime measurement.

3. The first $K^+\pi^-$ and $K^-\pi^+$ atom observation, its lifetime measurement and the $K\pi$ scattering length evaluation.

4. The investigation of Coulomb final state interaction in $\pi\pi$ and πK pairs.

The $\pi^+\pi^-$ and $K\pi$ scattering length are calculating in QCD.

K^+K^- atom.

The first step is investigation of K^+K^- pairs production in the effective mass region near $2m_K$

DIRAC set-up

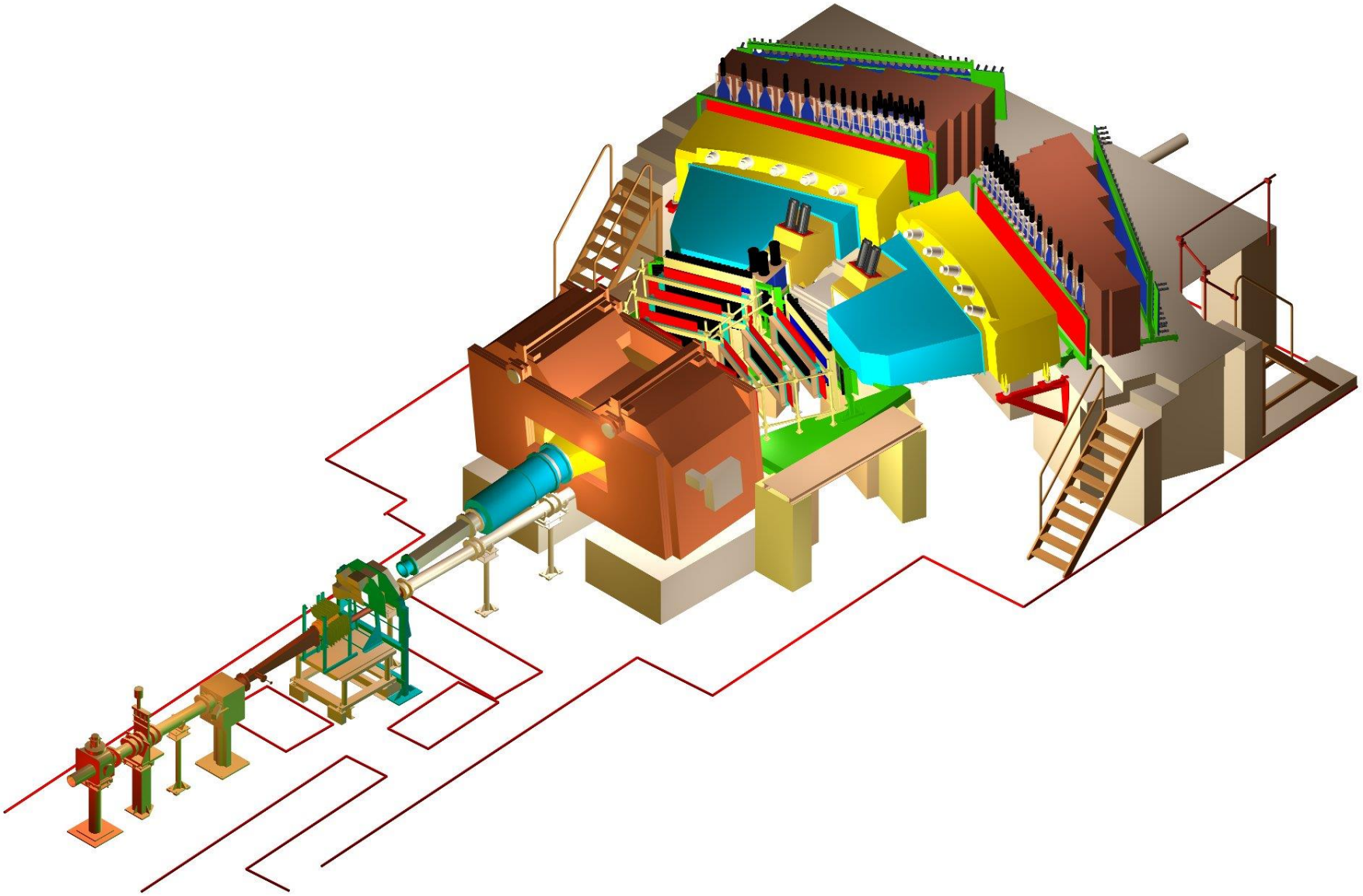

DIRAC set-up

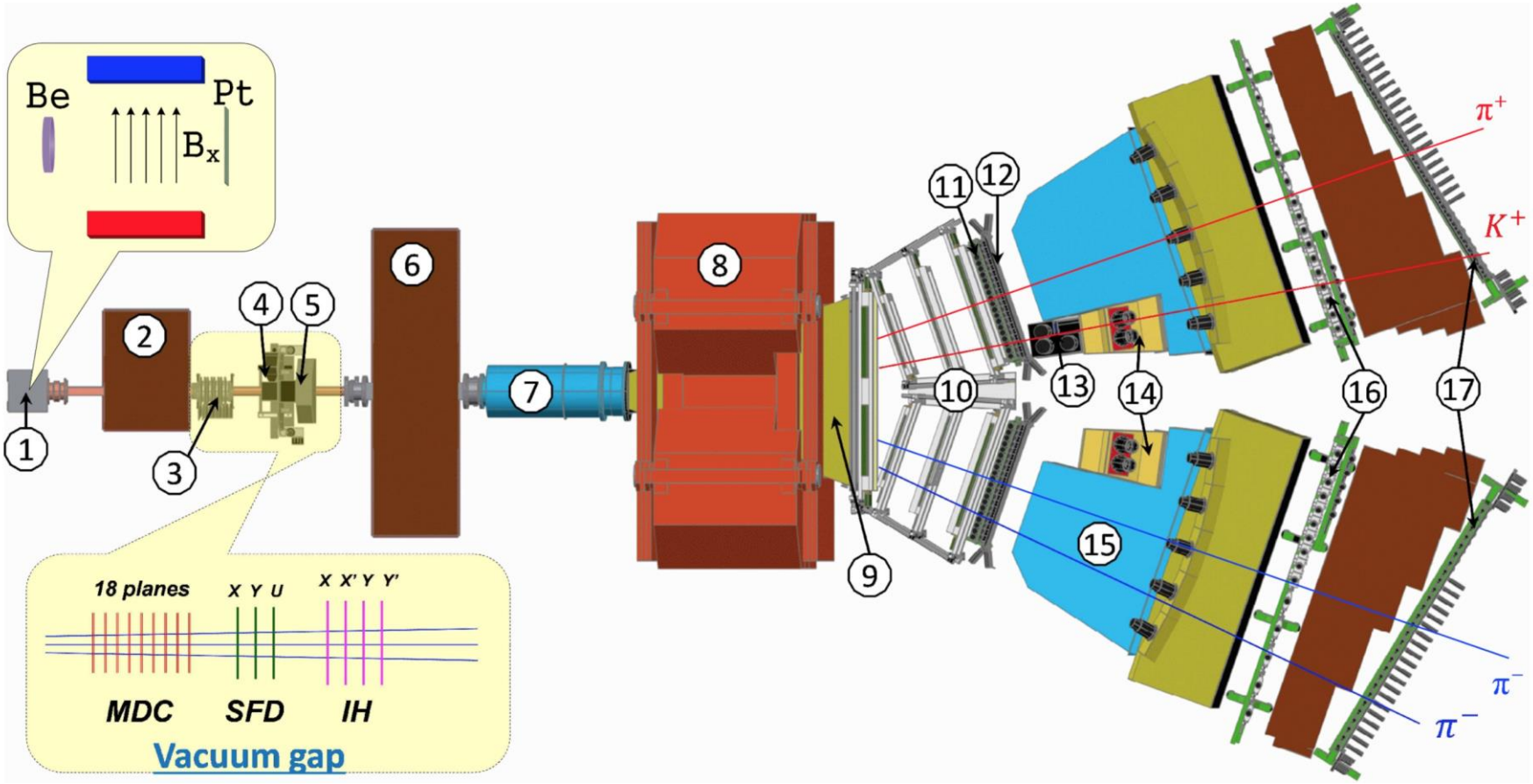

Fig. 2. General view of the DIRAC setup:
1 -- target station with insertion, showing the *Be* target, magnetic field and *Pt* breakup foil; 2 -- first shielding;
3 -- microdrift chambers (MDC); 4 -- scintillating fiber detector (SFD); 5 -- ionisation hodoscope (IH);
6 -- second shielding; 7 -- vacuum tube; 8 -- spectrometer magnet; 9 -- vacuum chamber; 10 -- drift chambers (DC);
11 -- vertical hodoscope (VH); 12 -- horizontal hodoscope (HH); 13 -- aerogel Cherenkov; 14 -- heavy gas Cherenkov;
15 -- nitrogen Cherenkov; 16 -- preshower (PSh); 17 -- muon detector.
(The plotted symmetric and asymmetric events are a $\pi^+\pi^-$ and $K^+\pi^-$ pair, respectively.)

Schematic description of K^+K^- production processes

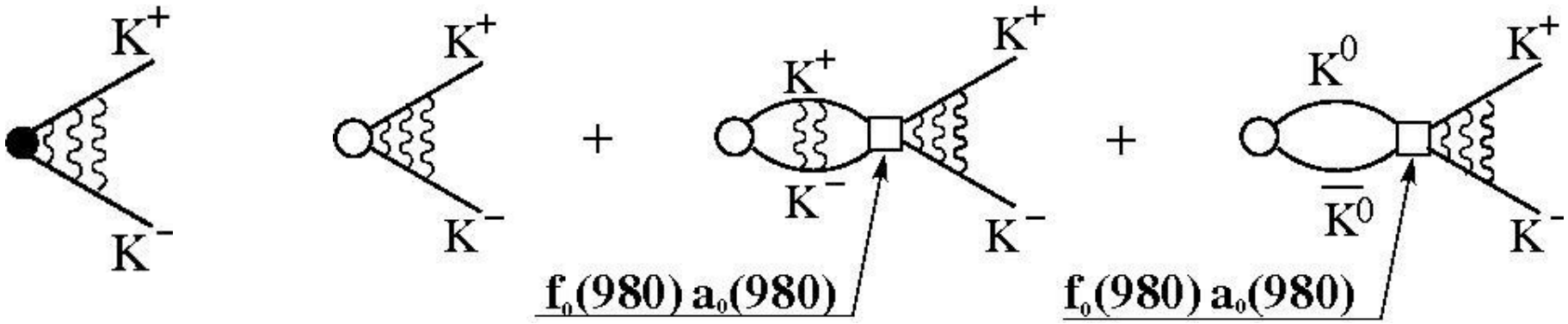

a) b)

Fig. 1

a) The black point presents the pair point-like production; the wavy lines describe the Coulomb interaction in the final state.

b) The circle and square present the pair non point-like production and strong interaction in the final state respectively.

Q_L distributions of the subsamples 30%, 50% and 70% for DATA3/ DATA2

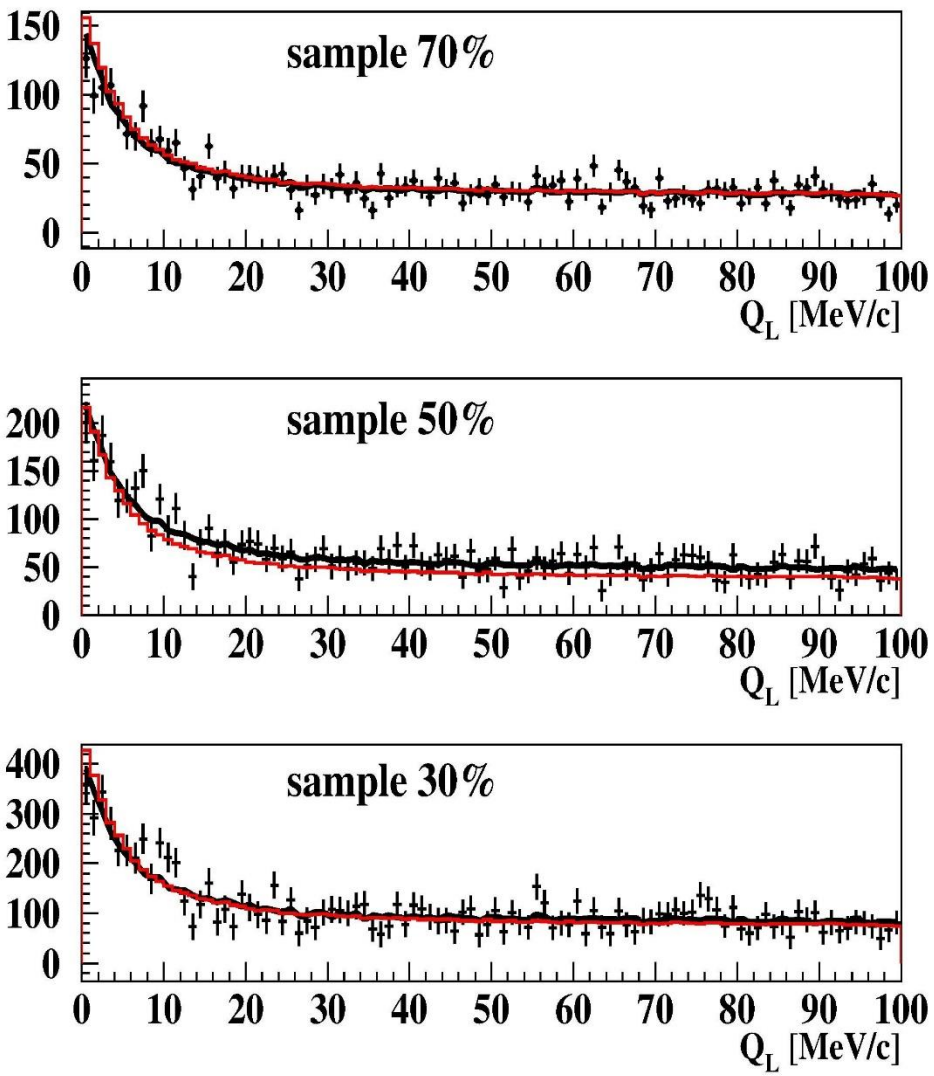

Fig. 2: The experimental spectra in the interval $0 < Q_L < 100$ MeV/c are fitted by simulated K^+K^- (point-like, Coulomb FSI) and residual $\pi^+\pi^-$ and p-anti-p background distributions. The red curve is the K^+K^- distribution, the black one is the sum of K^+K^- and residual background distributions. In the subsamples 70% and 30% the residual background is small and these curves practically coincide. For K^+K^- pairs in the region of $Q_L < 10$ MeV/c the Coulomb enhancement is clearly visible, whereas the residual background is small and practically uniform.

Matching pair numbers for Q and Q_L distribution analyses

	cut on ToF	distribution	K^+K^-	$\pi^+\pi^-$ & $p\bar{p}$ background
DATA2 + DATA3	70%	Q	3900 ± 410	-110
		Q_L	3930 ± 580	-140
	50%	Q	5320 ± 730	1100
		Q_L	5460 ± 1020	960
	30%	Q	11220 ± 1370	180
		Q_L	10750 ± 2020	300

The errors of K^+K^- and background values are the same.

It is seen from Table that the K^+K^- pairs number defined on Q and Q_L distributions do not differ significantly.

Q distributions of the subsamples 30%, 50% and 70% for DATA2 and DATA3

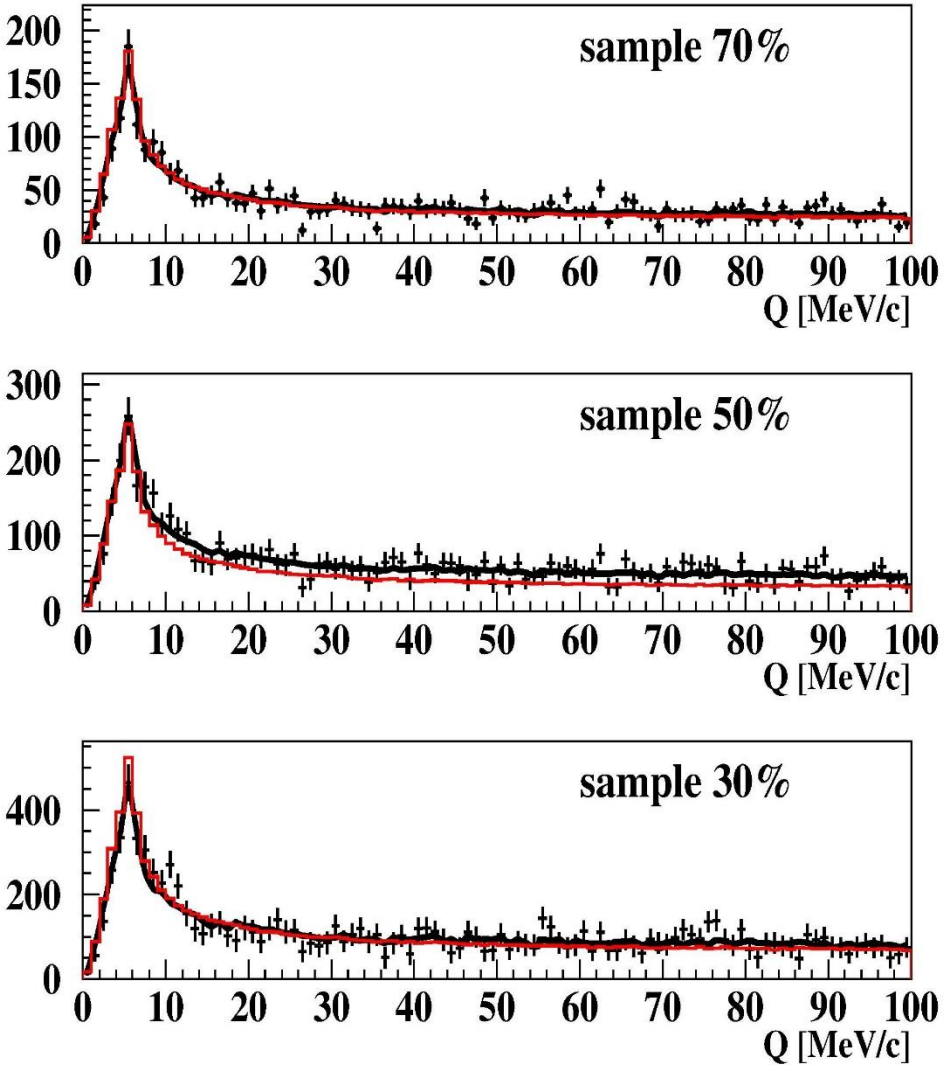

Fig. 3: Simulated distributions of K^+K^- (ALICE parame-trization) and residual back-ground of $\pi^+\pi^-$, accidental and p-anti-p pairs are fitting the experimental spectrum in the interval $0<Q<100$MeV/c. The red line is the K^+K^- distribution, the black line is the sum of K^+K^- and residual background. In the subsamples 70% and 30% the residual background is small and these lines practically coincide.

Q distributions in the interval 0-30 MeV/c of K^+K^-

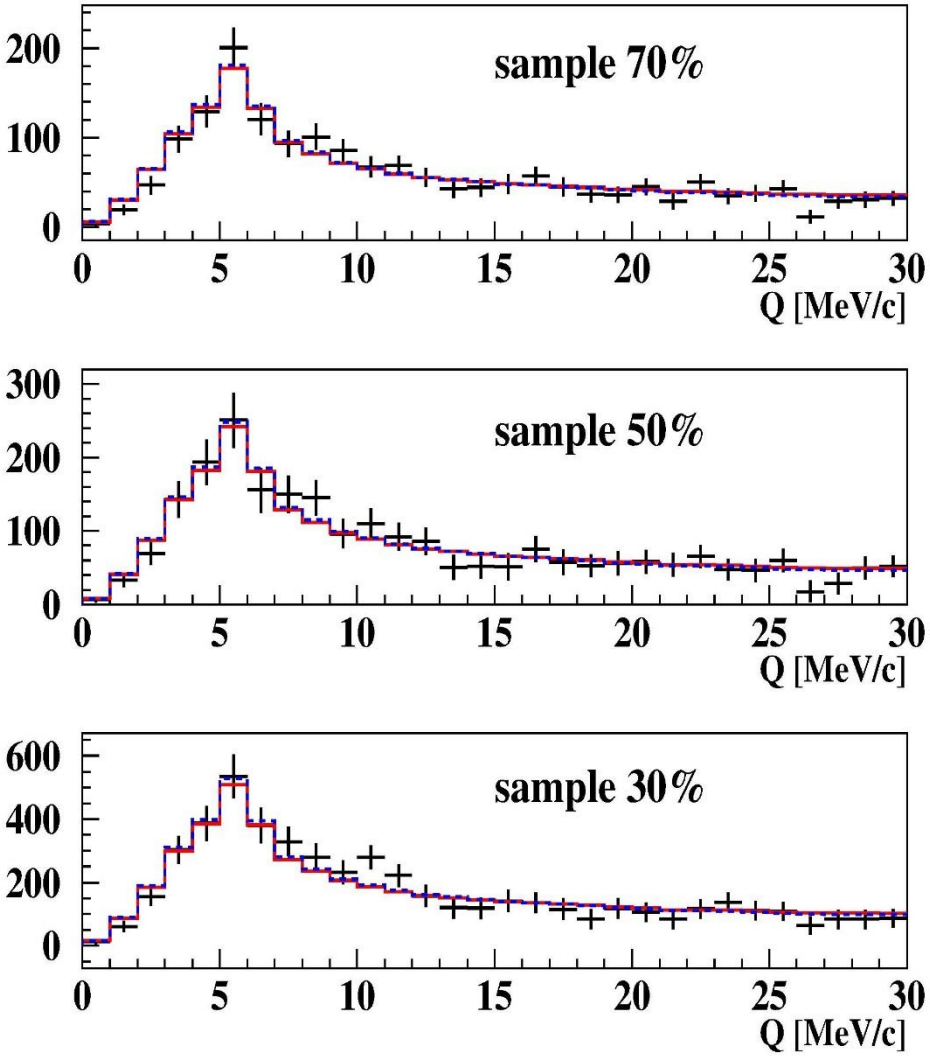

Fig.5 *Q* distributions in the interval 0-30 MeV/c of K^+K^- (ALICE parametrization) of the subsamples 30%, 50% and 70% for the DATA3/ DATA2 after residual background subtraction. The red and the blue fitting histograms were evaluated from the analysis of experimental distributions with residual background in Coulomb and Martin parametrizations respectively. It is seen that in this interval of *Q* the difference between these histograms is absent and they describe ”pure” experimental K^+K^- distributions well.

The first evaluation of the K^+K^- atoms number

The K^+K^- pairs analysis at Q_L < 30 MeV/c shows the Coulomb parametrization at small Q_L, describes well the experimental data, and confirm the Coulomb interaction as the main contribution to the final state interaction at small Q.

In this case, there is a direct connection between the detected number of K^+K^- pairs with small Q and the number of K^+K^- atoms generated in the experiment.

Based on experimental data, it allows, by a model independent way, to evaluate, in the first time, the number of produced K^+K^- atoms.

This work will begin in 2022.

KK Coulomb pairs and KK atoms

For charged pairs from short-lived sources and with small relative momenta Q, Coulomb final state interaction has to be taken into account. This interaction increases the production yield of the free pairs with Q decreasing and creates atoms.

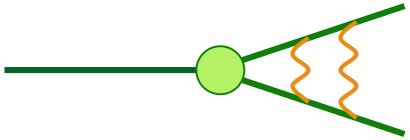

K^+K^-

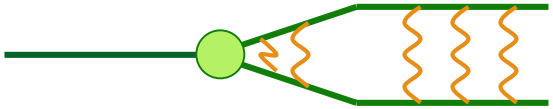

Coulomb pair

Atom

There is a precise ratio between the number of produced Coulomb pairs (N_C) with small Q and the number of atoms (N_A) produced simultaneously with Coulomb pairs:

$$N_A = K(Q_0)N_C(Q \le Q_0), \quad \frac{\delta K(Q_0)}{K(Q_0)} \le 10^{-2}$$

$$n_A - \textit{atomic pairs number}, \qquad P_{br} = \frac{n_A}{N_A}$$

The atom yields for DIRAC at 24 GeV/c and 450 GeV/c

p_p at θ_{lab}	$\pi^+\pi^-$ atom	$K^-\pi^+$ atom	$K^+\pi^-$ atom
p_p=24 GeV/c at θ_{lab}=5.7°	$190\cdot10^{-11}$	$22\cdot10^{-11}$	$52\cdot10^{-11}$
p_p=450 GeV/c at θ_{lab}=4.0°	$3400\cdot10^{-11}$	$810\cdot10^{-11}$	$850\cdot10^{-11}$
p_p=24 GeV/c at θ_{lab}=5.7° (DIRAC acceptance)	$120\cdot10^{-11}$	$1.3\cdot10^{-11}$	$3.1\cdot10^{-11}$
p_p=450 GeV/c at θ_{lab}=4.0° (DIRAC acceptance)	$1900\cdot10^{-11}$	$88\cdot10^{-11}$	$97\cdot10^{-11}$
yield ratio (DIRAC acceptance)	16	68	31

K^+K^- atom and its lifetime

Properties of the K^+K^- atom (kaonium or A_{2K}) [1]:

$a_B = [\alpha m_K/2]^{-1} = 109.6$ fm … Bohr radius

$p_B = \alpha m_K/2 = 1.80$ MeV … Bohr momentum

$|E_{1s}| = \alpha^2 m_K/4 = 6.57$ keV … binding energy

$\tau(A_{2K}) = [\Gamma(A_{2K})]^{-1} =$? … lifetime

The A_{2K} lifetime is strongly reduced by strong interaction (OBE, scalar f_0 and a_0) as compared to the annihilation of a purely Coulomb-bound system (K^+K^-).

K^+K^- interaction complexity ↓

τ ($A_{2K} \to \pi\pi,\pi\eta$)	K^+K^- interaction
1.2×10^{-16} s [2]	Coulomb-bound
8.5×10^{-18} s [3]	momentum dependent potential
3.2×10^{-18} s [2]	+ one-boson exchange (OBE)
1.1×10^{-18} s [2]	+ f_0' (I=0) + $\pi\eta$-channel (I=1)
2.2×10^{-18} s [4]	ChPT

References: [1] S. Wycech, A.M. Green, NPA562 (1993) 446;
[2] S. Krewald, R. Lemmer, F.P. Sasson, PRD69 (2004) 016003;
[3] Y-J Zhang, H-C Chiang, P-N Shen, B-S Zou, PRD74 (2006) 014013;
[4] S.P. Klevansky, R.H. Lemmer, PLB702 (2011) 235.

Proton-antiproton pairs analysis

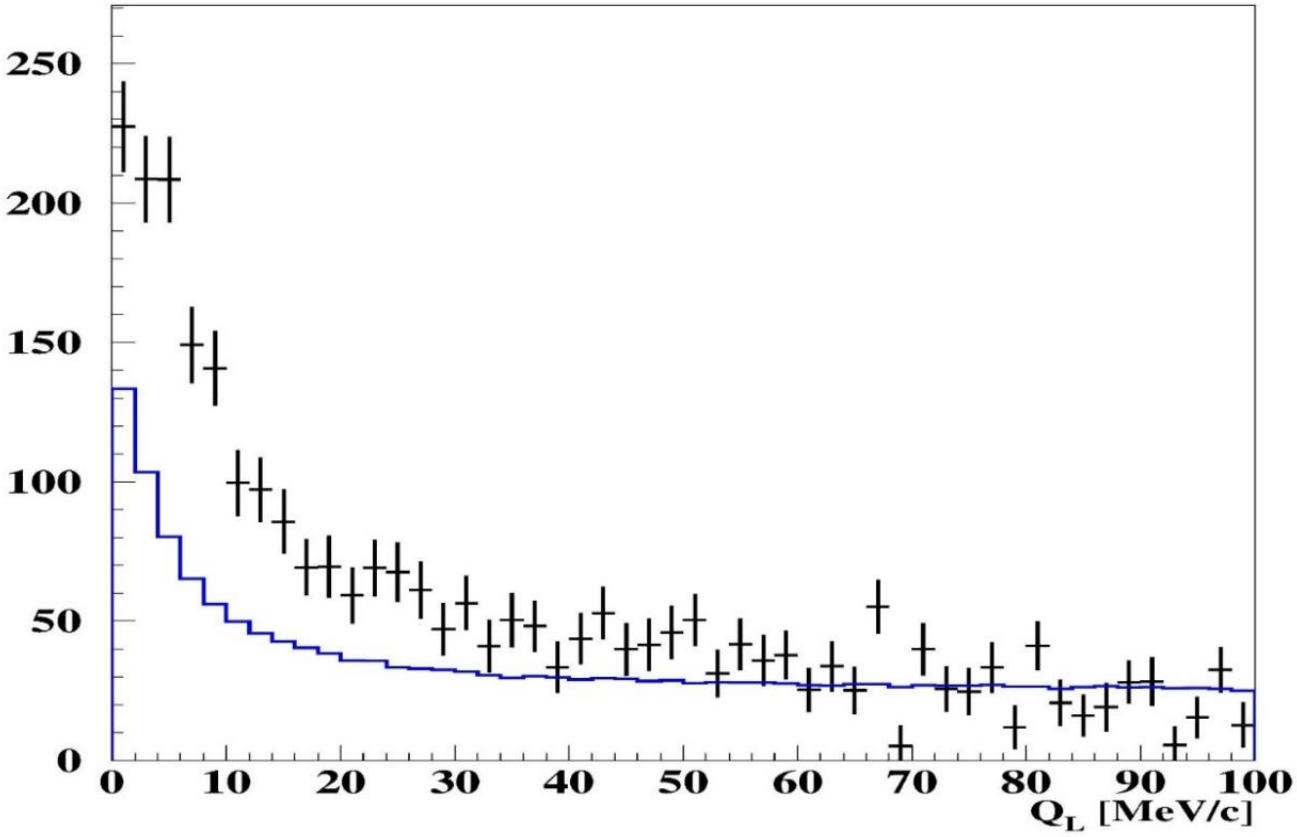

Fig. 6: Q_L distribution of pp^- pairs (black points). The blue histogram shows the K^+K^- pairs simulated spectrum calculated in the Coulomb parametrization and fitting experimental K^+K^- pairs distribution. This histogram fits the pp^- pairs distribution in Q_L interval 50MeV/c-100MeV/c. It is seen that for low Q_L values the Coulomb final state interaction enlarges the pp^- pairs yield significantly more than K^+K^- pairs.

Thank you

K^+K^- atoms ionization probability

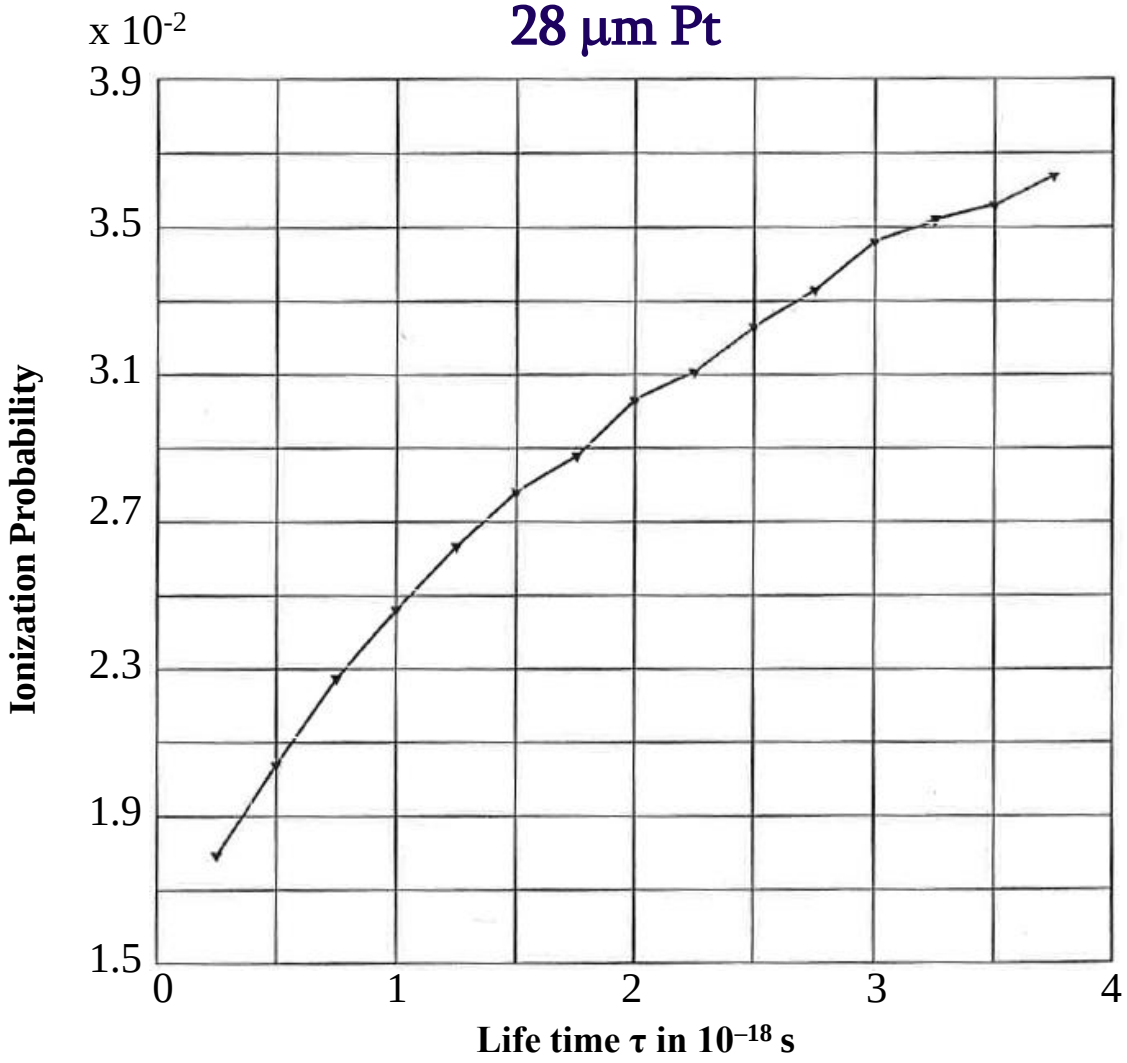

K^+K^- atoms Lorentz factor is $\gamma = 18$